

Non-generative Generalized Zero-shot Learning via Task-correlated Disentanglement and Controllable Samples Synthesis

Yaogong Feng, Xiaowen Huang*, Pengbo Yang, Jian Yu, Jitao Sang

School of Computer and Information Technology

& Beijing Key Lab of Traffic Data Analysis and Mining, Beijing Jiaotong University, China

{fengyg18, pengboyang, xwhuang, jianyu, jtsang}@bjtu.edu.cn

Abstract

*Synthesizing pseudo samples is currently the most effective way to solve the Generalized Zero Shot Learning (GZSL) problem. Most models achieve competitive performance but still suffer from two problems: (1) **Feature confounding**, the overall representations confound task-correlated and task-independent features, and existing models disentangle them in a generative way, but they are unreasonable to synthesize reliable pseudo samples with limited samples; (2) **Distribution uncertainty**, that massive data is needed when existing models synthesize samples from the uncertain distribution, which causes poor performance in limited samples of seen classes. In this paper, we propose a non-generative model to address these problems correspondingly in two modules: (1) **Task-correlated feature disentanglement**, to exclude the task-correlated features from task-independent ones by adversarial learning of domain adaption towards reasonable synthesis; (2) **Controllable pseudo sample synthesis**, to synthesize edge-pseudo and center-pseudo samples with certain characteristics towards more diversity generated and intuitive transfer. In addition, to describe the new scene that is the limit seen class samples in the training process, we further formulate a new ZSL task named the ‘Few-shot Seen class and Zero-shot Unseen class learning’ (FSZU). Extensive experiments on four benchmarks verify that the proposed method is competitive in the GZSL and the FSZU tasks.*

1. Introduction

The explosion of data and the rapid development of deep learning need massive precise but expensive labels. In the real world, these labels are usually sparse/missing, Zero Shot Learning (ZSL) techniques offer a good solution to address such problem, which trains on seen classes and tests on unseen classes (the seen classes and unseen classes are

*Corresponding author.

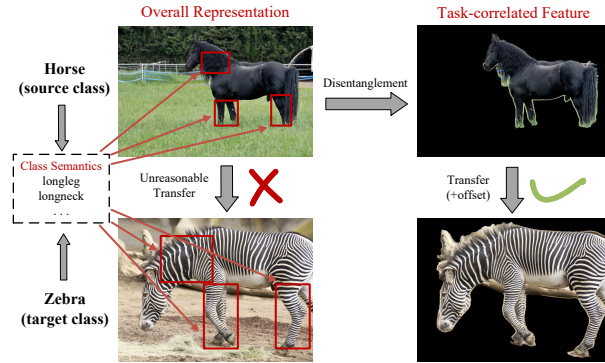


Figure 1. An illustration of core idea of our method. Different classes share class semantics. The images in the right half are the task-correlated features of the left half. They are excluded from task-independent features and are more consistent with class semantics, which is reasonable for the knowledge transfer in the GZSL task.

independent). In this paper, we focus on the Generalized ZSL (GZSL) task. It is a realistic setting of ZSL in making predictions on recognizing samples from both classes simultaneously rather than classifying only samples of the unseen classes.

At present, the method of synthesizing pseudo samples for unseen classes has proven to be one of the most effective ways of knowledge transfer to solve the GZSL problem. But there are still two challenging problems: (1) **Feature Confounding**. Most GZSL models are based on overall representations of samples extracted in pre-trained CNN (e.g., ResNet101 [13]) while the semantic features are class-level attributes or class-level sentence embeddings [21, 40]. The former contains more rich information and inconsistent with human cognition. So it is unreasonable to construct a mapping from visual features to semantic features directly and synthesize reliable pseudo samples based on the confounding visual features. Although some models [7, 23] contribute to extracting more human-consistent-cognition features, they are related to generative models and hard to

guarantee the diversity of sample synthesis with limited real samples.

(2) **Distribution Uncertainty.** The existed methods, especially the generative models, usually require a large amount of data to fit the distribution of real data, and can only synthesize pseudo samples with the uncertain distribution. So these models have poor performances when samples of seen class are few shot.

Figure 1 illustrates the motivation of our method. We first exclude the task-independent feature from horse image to horse object. Then we synthesize zebra’s pseudo samples of target class based on the horse’s task-correlated feature of source class in a non-generative way.

To be specific, we propose a non-generative approach named Task-correlated Disentanglement and Controllable Samples Synthesis (TDCSS) method that handles above issues. The TDCSS mainly consists of two components. (1) **Task-correlated Feature Disentanglement Module.** Our model is based on class semantic features to complete the image classification task. According to whether the visual features are corresponding to class semantics, we disentangle the confounding features into task-correlated features and task-independent features. The task-correlated features are more consistent with class semantics. We introduce the adversarial training of domain adaptation to achieve feature disentanglement. (2) **Controllable Pseudo Samples Synthesis Module.** Based on task-correlated features, we add different offsets to synthesize two types of pseudo samples which are edge-pseudo samples and center-pseudo samples in a non-generative way. For the edge-pseudo samples, we treat them as the adversarial examples in the feature-level and the edge offsets can be seen as perturbations in adversarial examples. For the center-pseudo samples, we make them distributed closer to the center of one class. Both of them guarantee the generative diversity of samples based on the limited seen samples. In addition, synthesizing pseudo samples with certain characteristics contribute to exploring the role of different types of pseudo samples in the knowledge transfer of GZSL.

To describe the scene that only has the limited samples on seen class in formulation, we further propose a new ZSL task named ‘Few-shot Seen class and Zero-shot Unseen class learning (FSZU)’. The FSZU is also more reasonable and more practical. In the GZSL task, all classes have strong semantic relationships. So we believe that the ZSL and the Few Shot Learning (FSL) are coexistent. For example, in the deep-space exploration and deep-sea exploration, the machine (detector) always encounter new situations, and the number of seen class samples that humans have obtained is also extremely limited. In this paper, we perform the TDCSS and the similar methods on the new task.

In summary, our main contributions of this work are

summarized as follows:

(1) We propose a novel non-generative model that disentangles visual features into task-correlated and task-independent by adversarial training of domain adaptation. And we use the task-correlated features to synthesize two types of pseudo samples as center-pseudo samples and edge-pseudo samples to guarantee the diversity of sample synthesis and the intuitive transfer.

(2) We propose a new zero shot task named ‘Few-shot Seen class and Zero-shot Unseen class learning (FSZU)’, which is more reasonable and more practical compared with the GZSL task in real life.

(3) Extensive experiments in the GZSL task and the FSZU task on four widely used datasets verify the results of the TDCSS are competitive with similar methods.

2. Related Works

2.1. Generalized Zero-Shot Learning

Domain shift is a basic problem in GZSL. It is described as ‘due to having disjoint and potentially unrelated classes, the projection functions learned from the auxiliary dataset/domain are biased when applied directly to the target dataset/domain’ [9].

GZSL with pseudo sample synthesis. Many researchers have proposed generative models to synthesize pseudo samples for unseen classes to alleviate this problem. The GAN-based models contribute to increasing the diversity of pseudo samples [22] and preserving semantic consistency [24, 30]. The VAE-based models [6, 19, 34] contribute to preserving semantic consistency of different representations of distribution in hidden layer. Some researchers integrate the VAE and GAN into a unified conditional feature generating model [29, 42] to integrate the advantages. There are also some non-generative models [8, 11, 12, 15, 26, 27] synthesizing pseudo samples. The models [15, 27] extract attribute-based features and then combine them to synthesize unseen pseudo samples. The BPL [11] synthesizes pseudo samples based on bidirectional projection learning and linear interpolation. The AGZSL [8] uses the Image Adaptive Semantics to expand the semantic features by using visual features, then it trains the seen class classifier based on the expanded semantic features and trains the unseen class classifier by synthesizing virtual class by sampling and interpolating over seen counterparts. The models [8, 11], synthesizing pseudo samples by perturbing or interpolating, are simpler and more likely to transfer class variations from seen class to unseen classes. So we use the non-generative models to synthesize pseudo samples.

GZSL with representation disentanglement. Most of GZSL models are based on the overall representations. Researchers use the representation disentanglement to obtain more consistent visual features with semantics. Some re-

searchers disentangle visual features into ‘object + attribute’ features [2, 28] by exploring their respective distributions. For example, the ‘red wine’ can be disentangled into ‘red (attribute)’ + ‘wine (object)’. But these methods require more strictly labeled datasets. Some researchers try to align attribute-based features with their attribute semantic vectors in fine-grained ZSL task [15, 16]. But their methods are based on the feature map at the last convolutional layer. Some researchers disentangle visual features according to their understanding of the GZSL. The DLFZRL [38] disentangles the feature into the semantic latent feature, the non-semantic latent feature, and the non-discriminative latent feature, in which the first two factors are learned by adversarial learning and the last is learned by a hierarchical structure. In addition, SP-AEN [5] disentangles the semantic space into two subspaces for classification and reconstruction respectively. Some researchers also use generative models with random permuting to achieve representation disentanglement [7, 23]. In this paper, we disentangle visual features into task-correlated features and task-independent features by using domain adversarial, which is more robust in different tasks.

2.2. Adversarial Example and Adversarial Self-Supervised Learning

Recently, extensive experiments [1, 33, 35, 39] have shown that model would have better generalization which has better adversarial robustness. And it achieves higher performance than the naturally trained models in ZSL [1]. These works usually use the gradient-based adversarial example generation algorithm, such as FSGM [10] and PGD [18]. Some self-supervised learning methods [14, 20] are also upgraded to adversarial self-supervised learning based on the adversarial examples in the way of contrastive learning, which extracts image features that are more consistent with human cognition.

In this paper, we draw on that core idea and further propose the edge-pseudo samples that can be seen as feature-level adversarial examples based on the targeted attack. We also introduce a training mechanism of the adversarial self-supervised to TDCSS to make our model extract more consistent task-correlated features with class semantics.

3. The Proposed Method

3.1. Problem Formulation

In the GZSL task, let $\{\mathcal{X}^s, \mathcal{Y}^s\}$ be the dataset with S seen classes, which contains N^s training samples $\mathcal{X}^s = \{x_{(i)}^s\}_{i=1}^{N^s}$ and the corresponding class labels $\mathcal{Y}^s = \{y_{(i)}^s\}_{i=1}^{N^s}$. The class labels span from 1 to S , $y^s \in L^s = \{1, \dots, S\}$. In the FSZU task, the $|S|$ is same with GZSL. But the samples on every seen class are much less than GZSL, which contains $\mathcal{X}^s = \{x_{(i)}^s\}_{i=1}^{N^f}$ and $\mathcal{Y}^s = \{y_{(i)}^s\}_{i=1}^{N^f}$, where

$N^f \ll N^s$. For the test set which involves unseen classes, the GZSL is the same as the FSZU. Specifically, given another dataset $\{\mathcal{X}^u, \mathcal{Y}^u\}$, on which the classes are related to the seen dataset. The dataset has U unseen classes and consist of N^u data instances $\mathcal{X}^u = \{x_{(i)}^u\}_{i=1}^{N^u}$ with corresponding labels $\mathcal{Y}^u = \{y_{(i)}^u\}_{i=1}^{N^u}$. The class labels thus range from $S+1$ to $S+U$, $y^u \in L^u = \{S+1, \dots, S+U\}$. The $L^s \cap L^u = \emptyset$. Each class is associated with a class-level semantic feature, which can be embedding and attribute. And the semantic information can be represented as $\mathcal{A} = \{a_{(k)}\}_{k=1}^{S+U}$. We denote \mathcal{A}^s and \mathcal{A}^u as the semantic features of seen and unseen classes. In this paper, the model training is achieved in two stages. We split the seen classes into source classes ($\{\mathcal{X}^{ss}, \mathcal{Y}^{ss}\}$, \mathcal{A}^{ss}) and target classes ($\{\mathcal{X}^{st}, \mathcal{Y}^{st}\}$, \mathcal{A}^{st}) in the first training stage. And we regard the seen classes as source classes and unseen classes as target classes in the second training stage.

3.2. Overall Framework

In this section, we present the details and the training strategy of TDCSS. The overall framework is illustrated in Figure 2. There are two key components: (1) **Task-correlated feature disentanglement**. We first disentangle the confounding visual features \mathcal{X}^s of source classes to task-correlated features h^{cor} and task-independent features h^{ind} by adversarial training of domain adaptation and making sure that both of them are precise, meaningful and independent to each other. The disentangled task-correlated features h^{cor} are then regarded as more reasonable representations for the sample synthesis. (2) **Controllable pseudo samples synthesis**. We use the task-correlated features h^{cor} of source classes to add the Center Offset o^{center} and the Edge Offsets o^{edge} respectively, which can synthesize two types of pseudo samples that are center-pseudo samples \hat{h}^{center} and edge-pseudo samples \hat{h}^{edge} . The offsets are outputted by convert networks.

3.3. Task-correlated Feature Disentanglement

This module is consists of adversarial training, reconstruction, and mutual minimization.

Adversarial Training. We aim to disentangle the visual features into h^{cor} and h^{ind} in an adversarial way.

In the classification training step, we input visual features \mathcal{X}^{ss} into Feature Extractor Network E , Task-correlated Network E_{cor} and Task-independent Network E_{ind} to disentangle the vectors into two factors. Then we train E , E_{cor} and E_{ind} in the supervised ways by using the compatibility loss which associates the visual and the semantic. The compatibility score function is parameterized by W , and is typically formulated as the bilinear compatibility function:

$$\tau_i^k = h_i W a_k \quad (1)$$

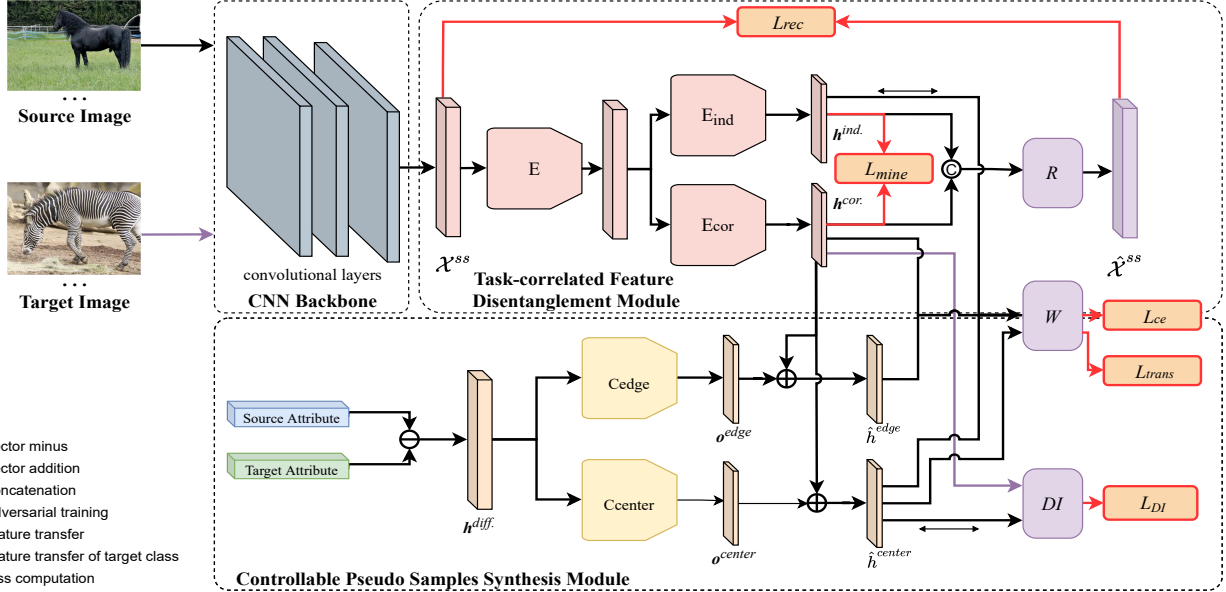


Figure 2. A schematic overview of TDCSS. The TDCSS is consist of two key component: (i) Feature Extractor Network E , Task-correlated Network E_{cor} and Task-independent Network E_{ind} , Reconstructor R , and W are set for Task-correlated Feature Disentanglement Module. The representation disentanglement of task-correlated features h^{cor} and task-independent features h^{ind} is achieved by adversarial training. And the independence between h^{cor} and h^{ind} and the meaningfulness of two factors are guaranteed by mutual minimization L_{mine} and reconstruction L_{rec} . (ii) The E , E_{cor} , W , Center Convert Net C_{center} , Edge Convert Nets C_{edge} , and Domain Identifier DI are set for Controllable Pseudo Samples Synthesis Module. The inputs of convert nets are the target semantic features minus the source semantic features. And offsets o^{center} and o^{edge} add h^{cor} of source images to synthesize center-pseudo samples \hat{h}^{center} and edge-pseudo samples \hat{h}^{edge} of target classes, respectively. The characteristics of \hat{h}^{center} is guaranteed by the transfer loss L_{trans} and the adversarial domain classification loss L_{DI} with h^{cor} of target visual features \mathcal{X}^{ss} .

where the h_i can be h^{cor} or h^{ind} of one sample after disentangling. And we further denote the attribute matrix:

$$\tau_i = h_i W \mathcal{A}^s \quad (2)$$

where the \mathcal{A}^s should be \mathcal{A} in the second training stage. We can consider τ_i as a classification score in the cross-entropy (CE) loss. So we further develop the compatibility loss function [43], which can be formulated as:

$$L_{ce} = \frac{1}{n_b} \sum_{i=1}^{n_b} L(\tau_i, y_i) \quad (3)$$

where the $L(\cdot)$ means the CE loss. The n_b means the size of one batch.

In the adversarial training step, we fix the parameter W of compatibility function and train E and E_{ind} to fool the classifier by minimizing the negative entropy of the predicted class distribution of h^{ind} outputted by E_{ind} .

Reconstruction. To guarantee the disentangled factors are meaningful, we reconstruct the confounding vector from them. Concretely, we concatenate h^{cor} and h^{ind} , and then input it into Reconstructor R to recover the confounding visual features \mathcal{X}^{ss} . Finally, the reconstruction loss function can be formulated as:

$$L_{rec} = \|\hat{\mathcal{X}}^{ss} - \mathcal{X}^{ss}\|_F^2 \quad (4)$$

where the $\hat{\mathcal{X}}^{ss}$ is the reconstructed vector of \mathcal{X}^{ss} , we use the L_{rec} to train R

Mutual Minimization. We need to make sure two factors are independent of each other. Concretely, we minimize the mutual information [3] between h^{cor} and h^{ind} in an unsupervised way. The mutual information minimization loss function can be formulated as:

$$\begin{aligned} L_{mine} &= \text{Mine}(h^{cor}, h^{ind}) \\ &= H(h^{cor}) - H(h^{cor}|h^{ind}) \\ &= H(h^{ind}) - H(h^{ind}|h^{cor}) \\ &= \sum_{h^{cor}, h^{ind}} p(h^{cor}, h^{ind}) \log \frac{p(h^{cor}, h^{ind})}{p(h^{cor})p(h^{ind})} \end{aligned} \quad (5)$$

where $H(\cdot)$ means the Shannon entropy and the $H(h^{cor}|h^{ind})$ means the conditional entropy of h^{cor} given h^{ind} . The $p(h^{cor}, h^{ind})$ means the joint probability distribution of (h^{cor}, h^{ind}) . We use the L_{mine} to train E , E_{cor} and E_{ind} .

3.4. Controllable Pseudo Samples Synthesis

This module is consists of pseudo sample synthesis and adversarial domain classification.

Pseudo Sample Synthesis. Firstly, we use the Center Convert Net C_{center} and the Edge Convert Nets C_{edge} to generate o^{center} and o^{edge} respectively. The inputs of these networks are the difference between semantic features of target classes and that of source classes. Then the corresponding offsets are further added to h^{cor} to synthesize \hat{h}^{center} and \hat{h}^{edge} of target classes respectively. This process can be formulated as:

$$\hat{h}^{center} = h^{cor} + o^{center} \quad (6)$$

$$\hat{h}^{edge} = h^{cor} + o^{edge} \quad (7)$$

where the o^{center} and o^{edge} can be further formulated as:

$$o_{ij}^{center} = C_{center}(a_i - a_j) \quad (8)$$

$$o_{ij}^{edge} = C_{edge}(a_i - a_j) \quad (9)$$

where i and j are the specific classes that from target classes and source classes respectively.

For different synthesizing samples, we have the following training process. Firstly, we use \hat{h}^{center} and \hat{h}^{edge} to train the C_{center} and the C_{edge} with classification loss in Eq. 2 and Eq. 3 by labeling as target classes. Furthermore, to guarantee \hat{h}^{center} distribute in the center of classes, we add the additional transfer loss to \hat{h}^{center} to train the C_{center} . The transfer loss is based on Eq. 2 and Eq. 3 but using the soft labels that are computed by cosine similarity of semantic features between source classes and target classes. Then, we introduce the adversarial self-supervised [20] that based on \hat{h}^{edge} to train the model. Concretely, for the \hat{h}^{edge} , the aforementioned process is similar to FSGM [10] algorithm and the offsets o^{edge} are similar to the perturbations in adversarial examples. We still label \hat{h}^{center} as target classes to train the parameters W of compatibility function by Eq. 2 and Eq. 3 while we label \hat{h}^{edge} as source classes. In this way, we can strengthen the model's adversarial robustness and further contribute to the generalization of the model.

Adversarial Domain Classification. We aim to synthesize pseudo samples more consistent with real samples which are achieved by adversarial domain classification. Specifically, we use the Domain Identifier DI , which takes \hat{h}^{center} and h^{cor} of \mathcal{X}^{st} as input and output the domain label l_f and $(1 - l_f)$ respectively. The loss function can be formulated as:

$$L_{DI} = -l_f \log(l_f) + (1 - l_f) \log(1 - l_f) \quad (10)$$

Then the C_{center} is trained by exchanging domain labels of real and pseudo samples to fool the DI . The \hat{h}^{edge} distribute between source classes and target classes, so we have not taken them into domain classification.

Table 1. The properties of datasets

	Dataset			
	AWA1	AWA2	CUB	FLO
#Samples	30475	37322	11788	8189
#Classes (train/test)	40/10	40/10	150/50	82/20
Attributes	85	85	1024	1024
Attribute value (Real or Boolean)	both	both	Real	Real

Table 2. Difference between our and compared methods (The details include Non-Generative Model (NGM), Soft Label (SL), Overall Feature (OF), Representation Disentanglement (RD), Pseudo Sample Synthesis (PSS))

Models	NGM	SL	OF	RD	PSS
DEM	✓	✗	✓	✗	✗
RELATION NET	✓	✗	✓	✗	✗
DCN	✓	✗	✓	✗	✗
TCN	✓	✓	✓	✗	✗
SP-AEN	✓	✗	✗	✓	✗
AREN+CS	✓	✗	✗	✗	✗
AGZSL	✓	✗	✓	✗	✓
f-VAEGAN-D2	✗	✗	✓	✗	✓
DLFZRL	✗	✗	✓	✓	✗
TDCSS	✓	✓	✓	✓	✓

3.5. Optimization and Unseen Samples Prediction

Our model is trained with different losses iteratively. In the second training stage, we regard the seen classes as source classes and unseen classes as target classes. We use the transfer loss to finetune C_{center} firstly and then synthesize \hat{h}^{center} of target classes to finetune W by Eq. 2 and Eq. 3. The first training stage and the second training stage are running alternately in one epoch.

Once the model training is completed, we can project the visual features into semantic space and measure the similarity with the semantic features of all classes in the GZSL task. Specifically, to predict the class label, the location of the maximum compatibility score can be chosen as the predicted label:

$$y = \arg \max_{k \in S+U} \phi(x)^T a_k \quad (11)$$

where $\phi(\cdot)$ includes the E , E_{cor} and the W .

4. Experiments

4.1. Experiments Setting

Datasets. We selected four popular datasets which are Animal with Attribute (AWA1) [21], Animal with Attribute2 (AWA2) [41], Caltech-UCSD Birds-200-2011 (CUB) [40] and Oxford 102 flowers (FLO) [31]. AwA1 and AwA2 are coarse-grained while others are fine-grained.

Table 3. Performance (in %) comparisons for GZSL in terms of unseen accuracy (u), seen accuracy (s), and their harmonic mean (H).

Methods	AWA1			AWA2			CUB			FLO		
	u	s	H	u	s	H	u	s	H	u	s	H
DEM [45]	32.8	84.7	47.3	30.5	86.4	45.1	19.6	57.9	29.2	57.2	67.7	62.0
RELATION NET [37]	31.4	91.3	46.7	30.0	93.4	45.3	38.1	61.1	47.0	50.8	88.5	64.5
DCN [25]	-	-	-	25.5	84.2	39.1	28.4	60.7	38.7	-	-	-
TCN [17]	-	-	-	61.2	65.8	63.4	52.6	52.0	52.3	-	-	-
SP-AEN [5]	-	-	-	23.3	90.0	37.1	34.7	70.6	46.6	-	-	-
AREN+CS [43]	-	-	-	54.7	79.1	64.7	63.2	69.0	66.0	-	-	-
AGZSL [8]	-	-	-	46.6	74.2	57.3	42.1	48.1	44.9	-	-	-
f-VAEGAN-D2 [42]	57.6	70.6	63.5	-	-	-	48.4	60.1	53.6	56.8	74.9	64.6
DLFZRL [38]	-	-	61.2	-	-	60.9	-	-	51.9	-	-	-
TDCSS	54.4	69.8	60.9	59.2	74.9	66.1	44.2	62.8	51.9	54.1	85.1	66.2

Table 4. Ablation study (in %) of the TDCSS components on AWA2 datasets in terms of unseen accuracy (u), seen accuracy (s), and their harmonic mean (H).

Setting	AWA2		
	u	s	H
TDCSS w/o TFD	52.7	74.4	61.7
TDCSS w/o EPS	44.5	71.9	55.0
TDCSS w/o CPS	34.9	79.3	48.4
TDCSS	59.2	74.9	66.1

The semantic features of CUB and FLO are from the CNN-RNN features [32, 44]. Our dataset split is under the PS setting [41]. The details are presented in Table 1.

Evaluation Metric. Average Class Accuracy (ACA) is adopted as the evaluation metric in the GZSL and FSZU tasks. We use the average per-class top-1 accuracy of unseen classes U and seen classes S to calculate the harmonic mean H :

$$H = \frac{(2 \times U \times S)}{U + S} \quad (12)$$

Comparison Methods. Since our model is a non-generative model, we mainly compare our proposed methods against current non-generative models. The main differences between compared methods and our TDCSS are shown in Table 2.

Implementation Details. We utilize the 2048D visual features extracted by pre-trained ResNet-101 [13]. The E , E_{cor} (E_{ind}), and DI consist of two-layer fully connected (FC) neural networks, in which the output units are 1800, 1024, and 2 respectively. The C , W , and R are three-layer FC neural networks, in which the hidden units are 1024, 512, and 1800. The output units of C are 1024. We use the LeakyReLU as the activation function for DI while the ReLU for others. Our model is implemented with PyTorch and optimized by ADAM optimizer. We set the learning rate as 2e-4 in the first training stage and 1/10 in the second training stage, epoch as 1500 for most. And in every epoch, we iterate 30 batches in the first training stage and 10 in the second training stage. Because of the limitation of sample

size on every class, the batch size is 32 for the FLO dataset and 64 for the other datasets. For source/target split in the first stage, we set the number of target classes to 2 for CUB and 1 for others.

4.2. Evaluations in GZSL Setting

The classification performances in the GZSL tasks are shown in Table 3. We observe that the TDCSS achieves competitive results on four datasets.

Compared with non-generative models, the H value of our model increases from 47.3% to 60.9% on AWA1, from 64.7% to 66.1% on AWA2, and from 64.5% to 66.2% on FLO. Specifically, the TCN contains the soft labels to quantify the transfer process in GZSL, which we add to \hat{h}^{center} synthesis process. It can be concluded that our model achieves improvement in addition to the transfer loss. The SP-AEN and AREN are based on tensor-level features. For the SP-AEN that tries to disentangle features, the experimental results prove our model is more effective. For the AREN+CS, our model is still competitive except on CUB dataset. However, the mechanism of calibrated stacking (CS) [4] helps the AREN achieve a great improvement in the GZSL task. But it is a post-processing operation and very susceptible to the influence of the parameter values that are manually set by the researchers. Our model does not use the CS but with comparable results, which shows TDCSS is more robust. For the AGZSL synthesized samples but with no representation disentanglement, which proves the effectiveness of representation disentanglement of our model.

Compared with generative models, the H value of our model increases from 60.9% to 66.1% on AWA2 and from 64.6% to 66.2% on FLO. However, the pseudo samples synthesized by our model have certain characteristics, which can further explore the role of different types of pseudo samples in GZSL knowledge transfer. The further detailed experiments are shown in section 4.3. The DLFZRL disentangles features by generative networks, our model also achieves comparable results generally but in a simpler concept and method.

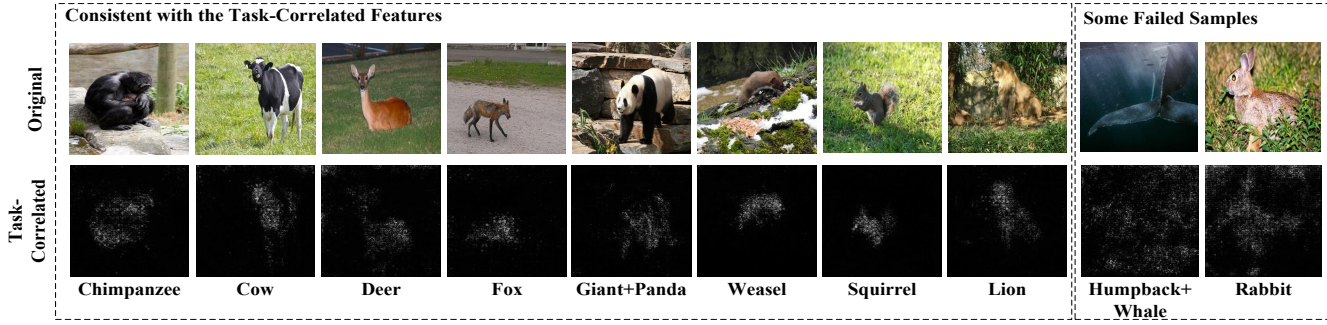


Figure 3. Visualization of task-correlated features that from AWA2 dataset by saliency maps

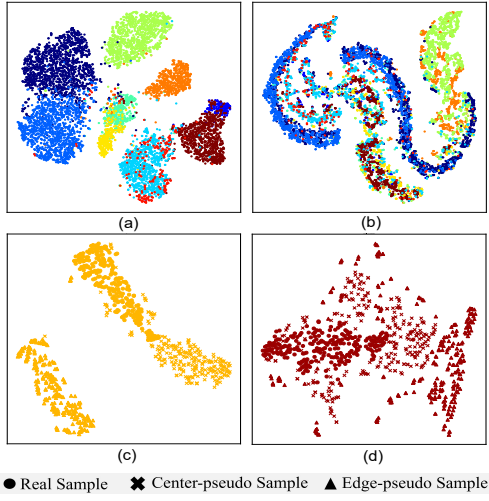


Figure 4. The t-SNE visual results of samples distributions on AWA2 dataset. (a) The task-correlated features h^{cor} . (b) The task-independent features h^{ind} . (c) & (d) The distributions of the real samples and different types of pseudo samples.

4.3. Ablation Study

We take the AWA2 dataset into the ablation analysis and aim to demonstrate that the main components of the TD-CSS both contribute to the final performance. We also observe the role of different types of pseudo samples in the knowledge transfer of the GZSL task. The best performance is achieved when TFD (Task-correlated Feature Disentanglement), EPS (Edge-Pseudo Samples) and CPS (Center-Pseudo Samples) are both applied. We have the following main findings:

(1) Compared with the model w/o TFD, it can be shown that disentanglement has little effect on the recognition of seen classes in the model, but has a greater impact on unseen classes. It proves that the disentanglement module, which extracts more consistent visual features with class semantics, is of great help to the knowledge transfer from the seen class to the unseen class.

(2) Compared with the model w/o EPS, the experiments

show that our whole model has a certain improvement in the accuracy of the seen and unseen classes, indicating that \hat{h}^{edge} with adversarial self-supervised training contribute to the consistency between h^{cor} and class semantics, and further improving the robustness and generalization of the model.

(3) Compared with the model w/o CPS, on the one hand, the precision on seen classes of the whole TDCSS is worse than it. It has demonstrated that \hat{h}^{edge} can further perfect the classification boundary for seen classes. On the other hand, the precision on unseen classes has significantly declined, it has proved \hat{h}^{center} play a key role in the knowledge transfer from the seen classes to the unseen classes in the GZSL task.

4.4. Qualitative Analysis

We take the AWA2 dataset into the following qualitative analysis.

Task-correlated features visualization We visualize h^{cor} and h^{ind} in Figure 4 (a) and (b) to validate the properties of the disentanglement. It shows that h^{cor} are much more discriminative than h^{ind} . But h^{ind} remain some discriminative, which we guess that some characteristics are not annotated in semantics. We further visualize h^{cor} by saliency maps [36] which compute the gradient of the output of E_{cor} against the original image inputted in the backbone network. The results are shown in Figure 3. We can observe that the saliency maps focus on the task-correlated information, especially the objects. And the task-independent information is effectively filtered. But there are also some failed samples that animals blend with their surroundings.

Distribution visualization of pseudo samples To demonstrate that our method can synthesize two types of pseudo samples effectively, we randomly select two classes and visualize the distributions of part samples. As Figure 4 (c) and (d) shows, we can observe that the distributions of \hat{h}^{center} are closer to real samples than that of \hat{h}^{edge} on the whole, which are consistent with their characteristics.

Table 5. Performance (in %) comparisons for FSZU in terms of unseen accuracy (u), seen accuracy (s), and their harmonic mean (H).

AWA2	All data			Num = 10			Num = 5			Num = 2		
	u	s	H	u	s	H	u	s	H	u	s	H
Disentangled-VAE [23]	50.9	79.8	62.2	50.8	64.7	56.9	39.2	58.1	46.8	29.8	39.7	34.1
SDGZSL [7]	74.4	63.6	68.6	47.1	53.3	50.0	25.7	56.1	35.3	6.8	39.9	11.6
AGZSL [8]	46.6	74.2	57.3	18.3	81.1	29.9	14.7	71.9	24.5	13.2	60.1	21.6
TDCSS	59.2	74.9	66.1	56.3	60.9	58.5	49.0	69.1	57.3	39.8	61.8	48.4
CUB	All data			Num = 10			Num = 5			Num = 2		
	u	s	H	u	s	H	u	s	H	u	s	H
Disentangled-VAE [23]	52.1	54.2	53.1	44.7	47.5	46.1	38.9	39.8	39.4	37.9	26.6	31.2
SDGZSL [7]	61.2	65.3	63.2	39.4	59.1	47.3	26.2	55.6	35.6	7.5	47.0	12.9
AGZSL [8]	42.1	48.1	44.9	29.3	42.9	34.8	21.7	36.1	27.1	13.7	26.8	18.1
TDCSS	44.2	62.8	51.9	40.1	54.5	46.2	43.4	45.5	44.4	34.5	38.1	36.2

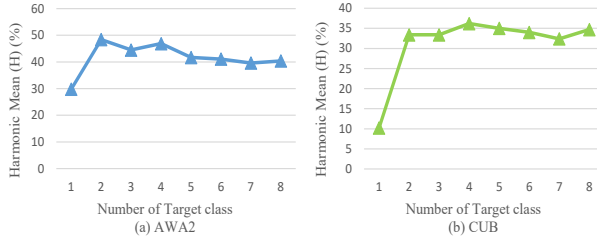


Figure 5. The experimental results under different numbers of target classes when the sample size of each class is 2.

4.5. Evaluations in FSZU Setting

For compared methods, we select two generative models that disentangle the overall representations into two factors by random permuting. The Disentangled-VAE [23] consists of two parallel VAEs and each with two branches. The SDGZSL [7] consists of VAE, AE, and the RELATION NET [37], while the VAE is used for data enhancement. We also select the non-generative AGZSL that synthesizes pseudo samples in mixup interpolation for comparison.

For experimental settings, we select AWA2 and CUB datasets, that appeared simultaneously in the Disentangled-VAE, SDGZSL, and AGZSL. And we reduce the sample size of seen classes (the sizes are set to 10, 5, and 2) to stimulate the FSZU. It should be pointed out that the Disentangled-VAE is reproduced by us based on Python 3.6 and Pytorch 1.0.1. For SDGZSL and AGZSL, we use the codes that have been released on Github. The performances in the FSZU tasks are shown in Table 5.

Compared with generative models, we achieve 22.4% improvement in H value on average for AWA2 and 8.8% for CUB. These experimental results reflect that our model can still work effectively in the new task. The generative model, especially SDGZSL, has excellent performances in GZSL but degrade sharply with the decrease in sample size, which shows more non-robust compared with our model. And our model can synthesize more diverse pseudo samples based on the limited seen class samples in a non-generative way.

Compared with the non-generative model that synthesizes pseudo samples, we achieve 117.9% improvement in H value on average for AWA2 and 65.5% for CUB. It shows that the representation disentanglement before synthesizing samples is reasonable and important. The results in the FSZU also show that the mixup interpolation of the AGZSL will lead the diversity of the synthesis samples to decrease sharply as the sample size decreases.

In the task of FSZU, we can improve the model’s performance by increasing the sample size of the target class with increasing the number of target classes. The results are shown in Figure 5. It shows that within a certain range, the accuracy will increase as the number of target classes increases, but too many target classes will cause the performance to decrease. It is a corollary that too many synthesized pseudo samples would be the leading data in the training process and further distract the model from recognizing real samples.

5. Conclusions

In this paper, we propose a non-generative model, TPDSS, to perform the task-correlated feature disentanglement and diversity pseudo samples synthesis in the GZSL and the FSZU tasks. For disentanglement, the TPDSS uses the adversarial training of domain adaptation to achieve it. For synthesis, the TPDSS synthesizes diverse pseudo samples with certain characteristics. The above mechanisms make our model achieve competitive performances in different tasks and help people intuitively understand the role of different types of pseudo samples in the knowledge transfer of ZSL.

Acknowledgments

This work is supported by the National Key R&D Program of China (Grant No. 2018AAA0100604), the National Natural Science Foundation of China (Grant No. 61832004, 61632002), and Beijing Natural Science Foundation (No.JQ20023).

References

- [1] Gunjan Aggarwal, Abhishek Sinha, Nupur Kumari, and Mayank Singh. On the benefits of models with perceptually-aligned gradients. *arXiv preprint arXiv:2005.01499*, 2020. 3
- [2] Yuval Atzmon, Felix Kreuk, Uri Shalit, and Gal Chechik. A causal view of compositional zero-shot recognition. *arXiv preprint arXiv:2006.14610*, 2020. 3
- [3] Mohamed Ishmael Belghazi, Aristide Baratin, Sai Rajeshwar, Sherjil Ozair, Yoshua Bengio, Aaron Courville, and Devon Hjelm. Mutual information neural estimation. In *International Conference on Machine Learning*, pages 531–540. PMLR, 2018. 4
- [4] Wei-Lun Chao, Soravit Changpinyo, Boqing Gong, and Fei Sha. An empirical study and analysis of generalized zero-shot learning for object recognition in the wild. In *European conference on computer vision*, pages 52–68. Springer, 2016. 6
- [5] Long Chen, Hanwang Zhang, Jun Xiao, Wei Liu, and Shih-Fu Chang. Zero-shot visual recognition using semantics-preserving adversarial embedding networks. In *Proceedings of the IEEE Conference on Computer Vision and Pattern Recognition*, pages 1043–1052, 2018. 3, 6
- [6] Xingyu Chen, Xuguang Lan, Fuchun Sun, and Nanning Zheng. A boundary based out-of-distribution classifier for generalized zero-shot learning. In *European Conference on Computer Vision*, pages 572–588. Springer, 2020. 2
- [7] Zhi Chen, Yadan Luo, Ruihong Qiu, Sen Wang, Zi Huang, Jingjing Li, and Zheng Zhang. Semantics disentangling for generalized zero-shot learning. In *Proceedings of the IEEE/CVF International Conference on Computer Vision*, pages 8712–8720, 2021. 1, 3, 8
- [8] Yu-Ying Chou, Hsuan-Tien Lin, and Tyng-Luh Liu. Adaptive and generative zero-shot learning. In *International Conference on Learning Representations*, 2020. 2, 6, 8
- [9] Zhenyong Fu, Tao Xiang, Elyor Kodirov, and Shaogang Gong. Zero-shot learning on semantic class prototype graph. *IEEE transactions on pattern analysis and machine intelligence*, 40(8):2009–2022, 2017. 2
- [10] Ian J Goodfellow, Jonathon Shlens, and Christian Szegedy. Explaining and harnessing adversarial examples. *arXiv preprint arXiv:1412.6572*, 2014. 3, 5
- [11] Jiechao Guan, Zhiwu Lu, Tao Xiang, Aoxue Li, An Zhao, and Ji-Rong Wen. Zero and few shot learning with semantic feature synthesis and competitive learning. *IEEE transactions on pattern analysis and machine intelligence*, 2020. 2
- [12] Yuchen Guo, Guiguang Ding, Jungong Han, and Yue Gao. Synthesizing samples fro zero-shot learning. IJCAI, 2017. 2
- [13] Kaiming He, Xiangyu Zhang, Shaoqing Ren, and Jian Sun. Deep residual learning for image recognition. In *Proceedings of the IEEE conference on computer vision and pattern recognition*, pages 770–778, 2016. 1, 6
- [14] Chih-Hui Ho and Nuno Vasconcelos. Contrastive learning with adversarial examples. *arXiv preprint arXiv:2010.12050*, 2020. 3
- [15] Dat Huynh and Ehsan Elhamifar. Compositional zero-shot learning via fine-grained dense feature composition. *Advances in Neural Information Processing Systems*, 33, 2020. 2, 3
- [16] Dat Huynh and Ehsan Elhamifar. Fine-grained generalized zero-shot learning via dense attribute-based attention. In *Proceedings of the IEEE/CVF Conference on Computer Vision and Pattern Recognition*, pages 4483–4493, 2020. 3
- [17] Huajie Jiang, Ruiping Wang, Shiguang Shan, and Xilin Chen. Transferable contrastive network for generalized zero-shot learning. In *Proceedings of the IEEE/CVF International Conference on Computer Vision*, pages 9765–9774, 2019. 6
- [18] Harini Kannan, Alexey Kurakin, and Ian Goodfellow. Adversarial logit pairing. *arXiv preprint arXiv:1803.06373*, 2018. 3
- [19] Rohit Keshari, Richa Singh, and Mayank Vatsa. Generalized zero-shot learning via over-complete distribution. In *Proceedings of the IEEE/CVF Conference on Computer Vision and Pattern Recognition*, pages 13300–13308, 2020. 2
- [20] Minseon Kim, Jihoon Tack, and Sung Ju Hwang. Adversarial self-supervised contrastive learning. *arXiv preprint arXiv:2006.07589*, 2020. 3, 5
- [21] Christoph H Lampert, Hannes Nickisch, and Stefan Harmeling. Attribute-based classification for zero-shot visual object categorization. *IEEE transactions on pattern analysis and machine intelligence*, 36(3):453–465, 2013. 1, 5
- [22] Jingjing Li, Mengmeng Jing, Ke Lu, Zhengming Ding, Lei Zhu, and Zi Huang. Leveraging the invariant side of generative zero-shot learning. In *Proceedings of the IEEE/CVF Conference on Computer Vision and Pattern Recognition*, pages 7402–7411, 2019. 2
- [23] Xiangyu Li, Zhe Xu, Kun Wei, and Cheng Deng. Generalized zero-shot learning via disentangled representation. In *Proceedings of the AAAI Conference on Artificial Intelligence*, volume 35, pages 1966–1974, 2021. 1, 3, 8
- [24] Bo Liu, Qiulei Dong, and Zhanyi Hu. Zero-shot learning from adversarial feature residual to compact visual feature. In *Proceedings of the AAAI Conference on Artificial Intelligence*, volume 34, pages 11547–11554, 2020. 2
- [25] Shichen Liu, Mingsheng Long, Jianmin Wang, and Michael I Jordan. Generalized zero-shot learning with deep calibration network. In *Advances in Neural Information Processing Systems*, pages 2005–2015, 2018. 6
- [26] Yang Long, Li Liu, Ling Shao, Fumin Shen, Guiguang Ding, and Jungong Han. From zero-shot learning to conventional supervised classification: Unseen visual data synthesis. In *Proceedings of the IEEE Conference on Computer Vision and Pattern Recognition*, pages 1627–1636, 2017. 2
- [27] Jiang Lu, Jin Li, Ziang Yan, Fenghua Mei, and Changshui Zhang. Attribute-based synthetic network (abs-net): Learning more from pseudo feature representations. *Pattern Recognition*, 80:129–142, 2018. 2
- [28] Ishan Misra, Abhinav Gupta, and Martial Hebert. From red wine to red tomato: Composition with context. In *Proceedings of the IEEE Conference on Computer Vision and Pattern Recognition*, pages 1792–1801, 2017. 3
- [29] Sanath Narayan, Akshita Gupta, Fahad Shahbaz Khan, Cees GM Snoek, and Ling Shao. Latent embedding feedback and discriminative features for zero-shot classification. *arXiv preprint arXiv:2003.07833*, 2020. 2

- [30] Jian Ni, Shanghang Zhang, and Haiyong Xie. Dual adversarial semantics-consistent network for generalized zero-shot learning. *arXiv preprint arXiv:1907.05570*, 2019. [2](#)
- [31] Maria-Elena Nilsback and Andrew Zisserman. Automated flower classification over a large number of classes. In *2008 Sixth Indian Conference on Computer Vision, Graphics & Image Processing*, pages 722–729. IEEE, 2008. [5](#)
- [32] Scott Reed, Zeynep Akata, Honglak Lee, and Bernt Schiele. Learning deep representations of fine-grained visual descriptions. In *Proceedings of the IEEE conference on computer vision and pattern recognition*, pages 49–58, 2016. [6](#)
- [33] Hadi Salman, Andrew Ilyas, Logan Engstrom, Ashish Kapoor, and Aleksander Madry. Do adversarially robust imagenet models transfer better? *arXiv preprint arXiv:2007.08489*, 2020. [3](#)
- [34] Edgar Schonfeld, Sayna Ebrahimi, Samarth Sinha, Trevor Darrell, and Zeynep Akata. Generalized zero-and few-shot learning via aligned variational autoencoders. In *Proceedings of the IEEE/CVF Conference on Computer Vision and Pattern Recognition*, pages 8247–8255, 2019. [2](#)
- [35] Ali Shafahi, Parsa Saadatpanah, Chen Zhu, Amin Ghiasi, Christoph Studer, David Jacobs, and Tom Goldstein. Adversarially robust transfer learning. *arXiv preprint arXiv:1905.08232*, 2019. [3](#)
- [36] Karen Simonyan, Andrea Vedaldi, and Andrew Zisserman. Deep inside convolutional networks: Visualising image classification models and saliency maps. 2014. [7](#)
- [37] Flood Sung, Yongxin Yang, Li Zhang, Tao Xiang, Philip HS Torr, and Timothy M Hospedales. Learning to compare: Relation network for few-shot learning. In *Proceedings of the IEEE conference on computer vision and pattern recognition*, pages 1199–1208, 2018. [6, 8](#)
- [38] Bin Tong, Chao Wang, Martin Klinkigt, Yoshiyuki Kobayashi, and Yuichi Nonaka. Hierarchical disentanglement of discriminative latent features for zero-shot learning. In *Proceedings of the IEEE/CVF Conference on Computer Vision and Pattern Recognition*, pages 11467–11476, 2019. [3, 6](#)
- [39] Francisco Utrera, Evan Kravitz, N Benjamin Erichson, Rajiv Khanna, and Michael W Mahoney. Adversarially-trained deep nets transfer better. *arXiv preprint arXiv:2007.05869*, 2020. [3](#)
- [40] Catherine Wah, Steve Branson, Peter Welinder, Pietro Perona, and Serge Belongie. The caltech-ucsd birds-200-2011 dataset. 2011. [1, 5](#)
- [41] Yongqin Xian, Christoph H Lampert, Bernt Schiele, and Zeynep Akata. Zero-shot learning—a comprehensive evaluation of the good, the bad and the ugly. *IEEE transactions on pattern analysis and machine intelligence*, 41(9):2251–2265, 2018. [5, 6](#)
- [42] Yongqin Xian, Saurabh Sharma, Bernt Schiele, and Zeynep Akata. f-vaeagan-d2: A feature generating framework for any-shot learning. In *Proceedings of the IEEE/CVF Conference on Computer Vision and Pattern Recognition*, pages 10275–10284, 2019. [2, 6](#)
- [43] Guo-Sen Xie, Li Liu, Xiaobo Jin, Fan Zhu, Zheng Zhang, Jie Qin, Yazhou Yao, and Ling Shao. Attentive region embedding network for zero-shot learning. In *Proceedings of the IEEE/CVF Conference on Computer Vision and Pattern Recognition*, pages 9384–9393, 2019. [4, 6](#)
- [44] Yunlong Yu, Zhong Ji, Jungong Han, and Zhongfei Zhang. Episode-based prototype generating network for zero-shot learning. In *Proceedings of the IEEE/CVF Conference on Computer Vision and Pattern Recognition*, pages 14035–14044, 2020. [6](#)
- [45] Li Zhang, Tao Xiang, and Shaogang Gong. Learning a deep embedding model for zero-shot learning. In *Proceedings of the IEEE conference on computer vision and pattern recognition*, pages 2021–2030, 2017. [6](#)